Enhancing Zone-Specific Rotator Cuff Enthesis Regeneration via Non-Cellular Extracellular Vesicle-Mediated MSC Differentiation

Zizhao Li[1], Yoon Ho Roh[1], Catherine Wang[1], Yujia Zhang[1], Jina Ko[1], and Su-Jin Heo[1]
[1]University of Pennsylvania, Philadelphia, PA

DISCLOSURES: Li (N), Roh (N), Wang (N), Zhang (N), Ko (N), and Heo (5-4WEB Medical)

INTRODUCTION: The rotator cuff is vital for shoulder movement and joint stability. However, tears at the rotator cuff enthesis site are very common **[1]**. Surgical interventions are often used, but re-tearing can happen due to scar tissue formation and insufficient vascularization at the repaired enthesis **[3-4]**. Furthermore, the intricate structure of the rotator cuff enthesis, segmented into distinct tendon, fibrocartilage, and bone zones, necessitates zone-specific approaches for effectively addressing its heterogeneity. Cell-based approaches have emerged to promote the healing of tendon and fibrocartilage phases within the enthesis. Notably, recent scientific focus has converged on extracellular vesicles (EVs), lipid-bound vesicles that carry variety of biological cargo, including RNAs, DNA, and proteins measuring ~30-200 nm in diameter **[5]**. Research has highlighted the substantial potential of EVs derived from various cell sources to enhance targeted delivery and improve therapeutic outcomes within the musculoskeletal domain **[6-7]**. For instance, extensive studies have corroborated that EVs sourced from tenocytes and mesenchymal stromal cells (MSCs) possess a remarkable capacity to induce tenogenic and chondrogenic differentiation **[8-10]**. Thus, this study aims to comprehensively characterize EVs extracted from distinct cell types: tenocytes (isolated from bovine Achilles tendons, T-EV) and mesenchymal stem cells (isolated from bovine bone marrow, MSC-EV). Further, we explore the impact of these EVs on recipient MSC proliferation and differentiation, thereby evaluating their therapeutic potential for zone-specific rotator cuff enthesis regeneration.

METHODS: To isolate EVs, juvenile bovine (< 3 months) tenocytes and MSCs (P1) were cultured in basal media until they reached approximately 90% confluency. T-EV and MSC-EV were then obtained by ultracentrifugation using our well-established protocol **[11-12]**. EV size distributions and total protein concentration were determined using nanoparticle tracking analysis (NTA). EV samples were stained with tetraspanin-specific fluorescent antibodies (CD63-568, and CD81-647) and subjected to super-resolution STORM imaging using an ONI Nanoimager microscope. The acquired STORM data underwent analysis through the Collaborative Discovery (CODI, ONI) online analytic platform to decipher the tetraspanin protein composition within the EVs. T-EV and MSC-EV were labeled with a lipophilic carbocyanine DiOC18 dye (DiO) to enable tracking of EV uptake in recipient bovine MSCs. Under EV-free pre-cultured conditions, two types of EVs were introduced to recipient MSCs at different concentrations (0-10k EVs/cell) to investigate how EVs isolated from two distinct cell types influence MSC proliferation and differentiation. On Day 3, fresh EVs were introduced alongside media replacement. Recipient MSC viability and proliferation were assessed by utilizing the Cell Counting Kit-8. On Day 7, TRIzol reagents were employed to isolate mRNA from the EV-recipient MSCs. Gene expression levels of tenogenic, and chondrogenic markers such as Type- I or II collagens (Col-1, Col-2) SOX-9, Tenascin C (TN-C), Aggrecan (ACAN)) were analyzed by RT-PCR, with GAPDH as the reference gene. Statistics was performed with ANOVA with Tukey's post hoc test.

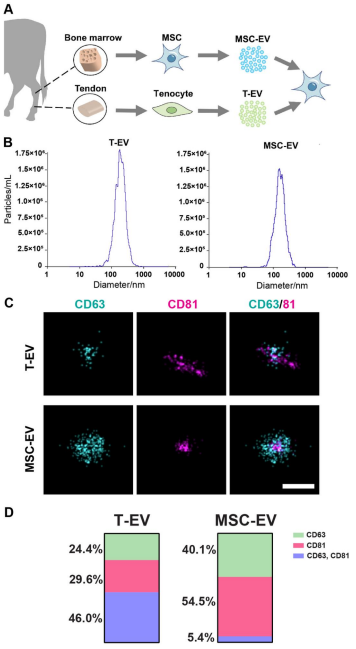

Fig. 1: (A) Schematic illustration of T-EV and MSC-EV isolation process and in vitro testing. (B) Quantitative NTA results. (C) Representative STORM images of individual T-EV and MSC-EV (Green: CD63, Red: CD81; scale bar = 200 nm). (D) Tetraspanin co-localization analysis of T-EV and MSC-EV.

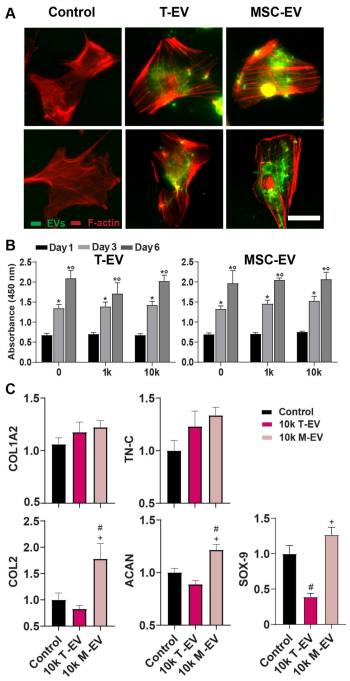

Fig. 2: (A) Representative fluorescence images of MSCs treated with EVs (bar = 50 μm). (B) MSC proliferation determined by CCK8 assay. [*: $p < 0.05$ vs. Day 1, ○: $p < 0.05$ vs. Day 3, n = 6/group, mean ± SD]. (C) Gene expression relative to GAPDH on Day 7 [#: $p < 0.05$ vs. Control, +: $p < 0.05$ vs. 10K T-EV, n = 6/group, mean ± SD].

RESULTS: Two distinct types of EV were successfully extracted and the NTA unveiled that T-EV and MSC-EV predominantly exhibited size distributions with mean sizes of 196.8 nm and 195.2 nm, respectively (**Fig. 1B**). Visual identification of T-EV and MSC-EV surface markers was accomplished by detecting the CD63/CD81 tetraspanins using STORM imaging at the individual levels (**Fig. 1C**). The significant enrichment of CD63 and CD81 tetraspanins and its ratio in EV membranes serve as a common indication of EVs and are employed as a biomarker for the detection of single-level EVs. Analysis in **Fig. 1D** demonstrated the existence of three different EV subpopulations in T-EV and MSC-EV: CD63 single-positive EVs, CD81 single-positive EVs, and CD63/CD81 double-positive EV subpopulations accounted for 46%, with relatively fewer single-positive subpopulations (CD63 only: 24.4%, CD81 only: 29.6%). Conversely, in MSC-EV, the dominant subpopulation consisted of CD81 single-positive EVs, comprising 54.5% of the total. CD63-positive EVs and double-positive EVs constituted 40.1% and 5.4% of the overall MSC-EV indicating two distinct EV populations. Representative fluorescence images exhibited the uptake of T-EV and MSC-EV by recipient bovine MSC, while no fluorescence was observed in the non-EV treated control group (**Fig. 2A**). The MSC proliferation rates remained consistent regardless of EV type and concentration (**Fig. 2B**), indicating the absence of EV-induced cytotoxicity. Interestingly, EV-treated MSCs demonstrated pronounce expression of tenogenic and fibrous markers (COL1A2 and TN-C) (**Fig. 2C**). MSC-EV treatment led to an enhancement in expression levels of chondrogenic gene (COL-2, ACAN, SOX-9) expression levels, while intriguingly showing a decrease with T-EV treatment (**Fig. 2C**).

DISCUSSION: This study has effectively examined the potential of bovine T-EV and MSC-EV to augment in vitro tenogenesis and chondrogenesis, presenting promising implications for the repair of the rotator cuff enthesis. Our approach encompassed a comprehensive characterization, including EV size determination, visualization of EV surface markers, and classification of distinct EV subpopulations. Notably, our findings indicated rapid EV uptake within 30 minutes, and the introduction of EVs to recipient MSCs did not lead to reduced cell proliferation rates when compared to the control group, underscoring the non-toxic nature and compatibility of EVs. Most intriguingly, the group treated with MSC-EVs exhibited heightened chondrogenic gene expression, while the T-EV treated group demonstrated diminished tenogenic/fibrogenic gene expression. These outcomes strongly propose the regulatory influence of distinct EV sources on gene expression. Moving forward, our study's trajectory will encompass the application of mass spectrometry and RNA sequencing to profile protein and RNA levels within both EV types. Concurrently, ongoing extended in vitro and in vivo investigations will ascertain the viability of EV therapy for the repair and regeneration of the rotator cuff enthesis. These cumulative efforts are poised to advance our understanding of EV-mediated interventions in musculoskeletal healing and underscore their therapeutic potential in clinical applications. **SIGNIFICANCE:** This study introduces a novel non-cellular EV-based approach that effectively promotes chondrogenic, tenogenic, and fibrous differentiation of MSCs. The implications of our findings extend to the promising potential for zone-specific regeneration and repair of the rotator cuff enthesis, particularly in combination with biomaterial systems.

REFERENCES: [1] Apostolakos+, *M.L.T.J.* 2014; [2] Sahoo+, *JSES Int.* 2015; [3] Sambandam+, *World J Orthop.* 2015; [4] Oh+, *Clin Orthop Surg.* 2018; [5] Nakase+, *Sci Rep.* 2016; [6] Zou+, *J. Nanobiotechnology* 2023; [7] Kodama+, *Bone Rep.* 2022; [8] Xu+, *CT.* 2019; [9] Yu+, *Acta Biomater.* 2020; [10] Connor+, *J. Bone Miner.* 2019; [11] Ko+, *Adv. Biosyst.* 2020; [12] Reynolds+, *J of Extracellular Bio.* 2023. **ACKNOWLEDGEMENTS:** This work was supported by the NIH (P50 AR080581, R56 HL163168) and NSF (CMMI-1548571).